

Performance of Low Cost Sensors Measuring Ambient Particulate Matter in High and Low Concentration Urban Environments

Karoline K. Johnson¹, Michael H. Bergin¹, Armistead G. Russell², Gayle S. W. Hagler³

¹School of Civil and Environmental Engineering, Duke University, Durham, NC, 27708, USA

5 ² School of Civil and Environmental Engineering, Georgia Institute of Technology, Atlanta, GA, 30332, USA

³ U.S. Environmental Protection Agency, Office of Research and Development, Research Triangle Park, NC, 27711, USA

Correspondence to: Karoline K. Johnson (Karoline.johnson@duke.edu)

Abstract. Air quality is a growing public concern in many countries, as is the public interest in having information on air pollutant concentrations within their communities. Quantifying the spatial and temporal variability of ambient fine particulate matter (PM_{2.5}) is of particular importance due to the potential health impacts associated with PM_{2.5}. This work evaluates three models of PM sensors (Shinyei: models PPD42NS, PPD20V, PPD60PV) in three locations: urban background (average PM_{2.5}: 8 $\mu\text{g m}^{-3}$) and roadside sites in Atlanta, Georgia, USA (average PM_{2.5}: 21 $\mu\text{g m}^{-3}$), as well as a location with substantially higher ambient concentrations in Hyderabad, India (average PM_{2.5}: 72 $\mu\text{g m}^{-3}$). Additionally, a low cost carbon dioxide (CO₂) sensor (COZIR GC-0010) and a mid-cost black carbon sensor (microAeth AE51) were tested at the roadside in Atlanta. Low cost sensor measurements were compared against reference monitors at all locations. The PPD20V sensors had the highest correlation with the reference environmental beta attenuation monitor (E-BAM) with R² values above 0.80 at the India site while at the urban background site in Atlanta, the PPD60PV had the highest correlation with the tapered element oscillating microbalance (TEOM) with an R² value of 0.30. At the roadside site, only the PPD20V was used, with an R² value against the TEOM of 0.18. Although the results of this work show poor performance under lower USA concentrations, the results indicate the potential usefulness of these low cost sensors, including the PPD20V, for high concentration applications up to approximately 250 $\mu\text{g m}^{-3}$. The CO₂ sensor had an R² value of 0.68 with the reference analyzer while the BC sensor correlated strongly to a multiangle absorption photometer (MAAP), with an R² of 0.99, at the Atlanta roadside site. These field testing results, although limited in nature, provide important insights into the varying performance of low cost particulate sensors used in highly contrasting atmospheric conditions and underlines the need to evaluate these emerging technologies, not only in the laboratory, but in their planned environment of application, prior to widespread use.

1 Introduction

Exposure to particulate matter (PM), particularly particles less than or equal to 2.5 micrometers in size (PM_{2.5}), is associated with a variety of adverse health impacts, including lung cancer (Laden et al., 2006), cardiovascular disease (Laden et al., 2006; Miller et al., 2007; Puett et al., 2009), and premature mortality (Puett et al., 2009). Although some cities in the US have PM values above the National Ambient Air Quality Standard (NAAQS) (EPA, 2013) annual PM_{2.5} concentration value of 12

$\mu\text{g m}^{-3}$, PM concentrations in many other countries, including India, are orders of magnitude higher (Tiwari et al., 2015; Health Effects Institute, 2010).

A variety of instruments are used for PM_{2.5} sampling. The US Federal Reference Method (FRM), is filter-based and non-continuous, and requires skilled personnel and highly specialized facilities and equipment to produce quantitative PM concentration values (EPA, 2015). Continuous measurement instruments, include US Federal Equivalent methods (FEMs) and other research grade instruments, often cost ten thousand to tens of thousands of dollars and usually need to be operated in climate-controlled spaces, with substantial oversight and maintenance (Chow, 1995). Many PM_{2.5} constituents vary within urban areas (Pinto et al., 2004), but the high costs associated with conventional measurements limit the number of air quality monitoring sites globally, leading to generally sparse spatially-defined air quality information that may not represent actual exposures (Stevens et al., 2014). Citizens and policy makers desire more data to make decisions for individual and societal health and well-being.

New sensor technologies may be able to address some of the issues of cost and convenience posed by conventional measurement equipment. New sensors are available that are lower in cost than their conventional counterparts, down to 1-10% of the cost of a reference analyzer. A further advantage is that these new sensors are small in size, light weight, and have minimal power consumption. These new sensors have been used to identify and monitor hot spots, and in arrays to generate data with higher spatial resolution (Gao et al., 2015), to collect personal exposure data (Nieuwenhuijsen et al., 2015; Steinle et al., 2015), to collect mobile monitoring data (Bossche et al., 2015), and a variety of other applications, including citizen science. Some sensors have been evaluated in lab conditions in addition to field conditions (Wang et al., 2015; Austin et al., 2015). The new sensors have the potential to be a feasible option for researchers, governments, citizens and community groups to monitor air quality in many more locations. Concerns remain about the accuracy and performance of these newer sensors due to their lower cost and more simplistic measurement techniques and because they often come with very little information from the manufacturer. This concern can be mitigated by thoroughly evaluating the sensors for specific applications and conditions (Snyder et al., 2013; Kumar et al., 2015).

The goal of this work is to evaluate several lower cost alternatives for generating continuous pollutant measurements in markedly different environments. These sensors include three models of particulate sensors, a carbon dioxide (CO₂) sensor, a black carbon (BC) monitor, and supporting temperature and relative humidity (RH) sensors. These PM sensors have been deployed both under low (USA) and high (India) ambient PM concentration settings.

2 Methods

2.1 Sensor Configurations

This research was conducted primarily through field studies designed to: (i) assess a sensor package capable of continuously measuring multiple air pollutants and (ii) characterize the performance of three commercially available, relatively low-cost optical particle sensors as well as a low cost CO₂ sensor and a mid-cost BC monitor compared to reference analyzers. After

assembly, the multi-sensor package was deployed in multiple field environments to examine how select sensors (Table 1) compared to reference monitors in ambient environments as well as to derive in situ emission factors along a major roadway. Three low-cost particle sensors were tested (PPD42NS, PPD20V, and PPD60PV, Shinyei Technology Co., Ltd. Kobe, Japan). The Shinyei sensors were selected because of their price and the prevalence of use of the PPD42NS and PPD60PV sensor in citizen science applications and custom-built research prototypes. The sensors measure particles using light scattering. An infrared LED is used as the light source, and a photodiode array with lens measures the scattered light at ~45 degrees. PM sensors provide an electrical signal (either analog or digital) based on light scattering, producing an output in units of voltage (analog), or ratio of time where a particle pulse was experienced (digital), with no manufacturer-specified equation to convert to PM concentration. The sensors have a 0.25 W resistor that is designed to heat the air, drawing a sample passively into the detection volume. The sensors measure the light scattering from a volume (as compared to single particle scattering) and therefore sampling is not a function of flowrate (as compared to single particle sensing) as long as the flow is not negligible enough to generate diffusional and/or settling losses in the sampling volume. The flow is generally maintained in the sensors by a heated resistor that generates air flow based on a thermal gradient.

All sensors were compared with either a Tapered Element Oscillating Microbalance (TEOM) (Thermo Scientific, USA) or an Environmental Beta Attenuation Monitor (E-BAM) (Met One Instruments, Grants Pass, OR, USA) to convert the electrical signal into PM concentration. Both reference analyzers were operated with PM_{2.5} inlet cyclones. Although the sensors are not size selective we have compared them against a PM_{2.5} reference since providing a surrogate measurement for PM_{2.5} is envisioned to be the common application for these low cost sensors.

The PPD42NS is a digital sensor: it provides a binary high or low output and sends pulses when particles are detected in the beam. These pulses are summed, and the fraction of time when pulses occur over the total time is calculated. In application, the researcher can use this ratio output from the PPD42NS to estimate particle mass concentrations by calibrating against a reference instrument. Previous work compared the Shinyei PPD42NS particle sensor to a variety of reference instruments both at US ambient concentrations (Holstius et al., 2014) and in Xi'an, China, at higher ambient concentrations (Gao et al., 2015) and have also been evaluated in lab experiments (Austin et al., 2015; Wang et al., 2015).

The other two Shinyei sensors (PPD20V and PPD60PV) have an analog output, with a variable voltage depending on the light scattering occurring in the sensing volume. These sensors also have the capability to function as digital sensors but were not used in this way for our experiments. The manufacturer reports that the PPD42NS and PPD20V detect particles greater than 1 µm in size (Shinyei Kaisha, 2002; Shinyei Technology Co., 2010) while the PPD60PV detects particles greater than 0.5 µm in size (Shinyei Technology Co., 2013). Unfortunately, Shinyei Technology Co. has provided no further information regarding the design of these three sensors. These particle size ranges appear to be somewhat arbitrarily defined by the manufacturer and little information is provided on their evaluation.

A relationship between electrical output and PM mass concentration was generated for all three types of sensors in the field using linear and orthogonal regression. First the sensors were calibrated using linear regression and then orthogonal regression

was applied to reduce the errors in both the X and Y directions. The first step (applying linear regression) is important as orthogonal regression assumes equal error in both directions and this will be an especially poor assumption if the sensors are on different scales. In some cases an exponential function was applied instead, in the case of non-linear saturated results. These relations were computed using the one hour averages of the sensor and the reference analyzer except in the laboratory evaluations where one minute data were used. The standard deviation of the error, the difference between reference analyzer and generated sensor concentration, was also estimated (s_d). Applying orthogonal regression, instead of linear regression alone, reduces the s_d by up to a few $\mu\text{g m}^{-3}$. The 95% confidence interval of the error is $1.96s_d$, meaning that the error between the sensor estimate is within $1.96s_d$ of the reference instrument 95% of the time.

In addition, a low power, 3.5 mW, nondispersive infrared (NDIR) (CO2Meter.com) CO₂ sensor was used. The sensor was calibrated for a range of 0-1025 ppm in the laboratory prior to deployment and was recalibrated against a CO₂ instrument (Thermo Fisher Scientific Inc. Franklin, MA, USA 410i) in the field using linear regression of the one hour averages of the sensor and the reference analyzer. In addition, a mid-cost, portable black carbon monitor was added to the sampling package (microAeth, AE51, Aethlabs, San Francisco, CA, USA). The performance of the microAeth as compared to reference Multiangle Absorption Photometer (MAAP) and Aetholometers has been characterized in previous papers (Cheng and Lin, 2013; Viana et al., 2011). Adding a low-cost CO₂ measurement to sensor packages is potentially powerful in that such measurements can be used in concert with PM measurements (i.e. PM_{2.5} and black carbon concentrations) to estimate emissions factors (EF). In conjunction with the other sensors, a Sensiron AG (Stäfa, Zurich, Switzerland) temperature and relative humidity (RH) sensor (SHT15) that measured temperature by band-gap displacement and RH using a capacitive sensor (Sensiron, 2010) was used to measure environmental conditions within the sampling enclosure. RH measurements are especially important with the use of light scattering PM sensors. Based on past work characterizing the change in light scattering coefficient as a function of RH for anthropogenic aerosol it is expected that water uptake on aerosol particles will result in an increase in the light scattering coefficient of 10%-30% at an RH of 70% RH, and 40%-70% at an RH of 80% (Rood, 1987; McInnes et al., 1998). Therefore higher RH measurements may result in overestimates of PM mass by the sensors since the reference measurements are for dried aerosol and do not reflect substantial amounts of water mass.

Other than the microAeth, which has internal data logging, these sensors were wired to an Arduino Mega microcontroller (Arduino, www.arduino.cc, last accessed September 14, 2015) which was paired with a data logging shield (which includes a real-time clock) from Adafruit (New York, NY, USA) that logged the sensor's analog signal or pulse ratio and stored time stamped one-minute averages to comma-separated values (CSVs) on an SD card. These sensors were assembled into opaque plastic junction boxes. Figure 1 shows a 6" x 6" x 4" box with sensors used during the roadside testing. The box and additional electronics to run these sensors cost just over \$100 from a local hardware store and online suppliers. A 25 mm fan was positioned to draw air in to the instrument package and was positioned directly below the PM sensor. This was added to improve air flow through the sensor so that the sensors would be able to sample external air since the heating resistor would only supply flow through the individual PM sensors and not through the whole box. The air flow volume for the fan, as reported by the manufacturer, was 67 liters per minute so the exchange rate in the junction box is estimated to be approximately twice

per second in the case of the roadside site. The exhaust flowed out the elbow on the right hand wall of the box, and the instrument cables were threaded through the elbow as well. A slightly different setup was used for the sensor comparison testing where multiple PM sensors were operated at the same time (Figure 2). In this case, three 25 mm fans were positioned to draw air in to the instrument package and again, the exhaust flowed out an elbow. Four of the PM sensors, the three PPD20V sensors and the PPD60PV, were positioned directly above the fans. The PPD42NS was placed on the wall of the box perpendicular to the other sensors as shown in Figure 2. The three fans provided ample flow through the PPD42NS and the CO₂ and temperature/RH sensors although not directly adjacent. Placing the PPD42NS further from the fan inlet allowed it to be further from the fan opening where stray light could enter and influence the results. This is more important for the PPD42NS since it has a more open light scattering chamber than the other two sensors. With three fans, the exchange rate in the junction box was estimated to be approximately six times per second for the comparison box, although possibly less due to flow resistance through the box. Given that the sensors measure the light scattering from a volume it is not expected that the estimated PM concentrations are a function of flowrate, although it is possible that particles losses, particularly for larger coarse particles that can impact on surfaces within the sampling box, are influenced by the flow rates. We did not assess the dependence of air flow on particle losses, and an assumption is that fine particulate mass concentrations for the flow rates reported here are not influenced by particle losses.

2.2 Sensor Evaluation

Particle properties are variable and are composed of both internal and external mixtures of chemical components that vary as a function of size. The response of optically-based PM sensors is largely a function of the actual properties of the ambient aerosol at the specific measurement location, including the size distribution and chemical composition. Lab studies with light scattering particle sensors have found the responses vary by a factor of 10-12 depending on particle size and composition (Wang et al. 2015, Austin et al. 2015). While laboratory evaluation is useful, there are limitations in the ability to generate aerosol mixtures that match the variability of chemical and physical composition of particles in urban environments. This work focuses mainly on field evaluations of sensors against reference monitors, rather than laboratory studies to evaluate sensor response as a function of particle size, composition, and concentration that is not representative of field conditions. However, we do discuss evaluations conducted in our laboratory as well as recent detailed laboratory analyses of similar sensors (Wang et al., 2015; Austin et al., 2015).

2.2.1 Field Evaluation: Sampling locations and reference instruments

Three field evaluations with reference analyzers were carried out (Table 2). The Thermo Scientific Series 1400a TEOM, with a PM_{2.5} cyclone, was used as the reference for the two Atlanta sampling periods. The TEOM is a US EPA Federal Equivalent Method (FEM) at a 24-hour averaged level and is used routinely for regulatory and research monitoring (EPA, 2015). A high efficiency particle arresting (HEPA) filter was attached at the inlet on the TEOM periodically to ensure that there were no

leaks in the sampling line. Data and any instrument error flags were reviewed periodically and that the instrument was functioning properly. An E-BAM also with a PM_{2.5} inlet, was the reference instrument used in Hyderabad, India. An E-BAM is a more portable monitoring option than a traditional BAM, operating in the environment without requiring an exterior enclosure (Met One Instruments, 2008). The E-BAM is not a registered FEM in the U.S., although the instrument strongly correlates with federal reference methods (USDA Forest Service, 2006) and has been used as a reference instrument in past studies (Ancelet et al., 2012). Periodic leak checks, flow checks, and monthly nozzle/vane cleanings were performed to ensure proper function of the E-BAM.

Measurements from three different sampling locations (an urban background in Atlanta, a roadside in Atlanta, and a location in Hyderabad, India) were analyzed in this study. The first measurement campaign was at the side of the freeway on the Georgia Tech campus, Atlanta, GA, (33.775560, -84.390950), adjacent to a 15-lane freeway with an Average Annual Daily Traffic (AADT) of 293,256 vehicles in 2014 (Interstate 75 & 85) (GDOT, 2014). The sensor box (Figure 1) was mounted onto a pole on top of a trailer approximately 4 meters above ground. The trailer was parked in a lot separated from the highway by only a fence, leaving the sensor package approximately 6 m from the closest lane of traffic. The TEOM inlet was within a few feet of the sensor package. Next, a comparison was performed on the roof top of the Ford Environmental Science and Technology Building, a four-story building on the Georgia Tech campus, approximately 500 m from the freeway (33.779175, -84.395730). The rooftop, urban background site was above the tree level but there were a few structures on the roof such as an indoor roof top laboratory and building air handling equipment. The inlet of the TEOM and the sensors were located within about 3 meters of each other. Lastly, the same sensor package that was deployed on the Atlanta roof top was deployed in Hyderabad, India (17.425798, 78.526814). The sensor package was deployed on a roof top at the National Institute of Nutrition (NIN). The sensor package was attached to the E-BAM stand so they were measuring in the exact same location.

The selection of these three sites gives us a variety of concentration ranges to help determine appropriate uses of the sensors. For sensors that showed at least a correlation of 0.32 ($R^2 > 0.1$), orthogonal regression was applied to the one-hour averaged data to convert the raw voltage output from the PM sensors into an estimated PM_{2.5} mass concentration (Table 3). Orthogonal regression reduces errors in both the x and y directions and is used since there is variability not only in the sensors but also in the reference instruments on this one-hour time scale. For the roadside evaluation, the calibration was generated using data from the whole period since sampling occurred over 3 days. During Hyderabad the first half of the data were used to generate a calibration that was then applied to the second half of the data.

2.2.2 Laboratory evaluation

A chamber experiment was also run with the 3 PM sensors. A 284 liter modified sealed glovebox with a slight positive pressure was used. A puff of incense smoke was introduced into the chamber and the concentration was allowed to decay while clean air was pumped into the chamber. Over a 1-hour period the concentration dropped from above 500 to 0 $\mu\text{g m}^{-3}$ as measured by a TSI DustTrak 8533 (Shoreview, MN) (Figure 9). The sensors were located inside the chamber while a line ran from the

chamber with a short length of antistatic tubing going to the DustTrak and another exhausted through a filter and into the lab. The correlation between the 3 sensors and the DustTrak determined and is discussed in the text.

3 Results and discussion

Results from these three measurement periods characterize a wide array of atmospheric conditions and different urban surroundings, as well as differences due to source contributions (Table 3). The results have also been compared to results from lab evaluations from this work (Table 5) and previous lab evaluations.

3.1 Ambient concentration comparisons

3.1.1 Urban Roadside

The first measurement campaign was at the side of the freeway on the Georgia Tech campus. Reference PM_{2.5} readings ranging from fairly low ($\sim 10 \mu\text{g m}^{-3}$) to moderate (maximum of $32 \mu\text{g m}^{-3}$) concentration levels. Previous work comparing light scattering from a nephelometer (Radiance Research Inc., M903 nephelometer) to a TEOM in urban Atlanta found a clear link between light scattering coefficient and PM_{2.5} ($R^2=0.8$) (Carrico et al., 2003) with roughly 60% of the light scattering by particles greater than 0.5 μm . However, the roadside comparison between the TEOM and the Shinyei PPD20V sensor provided a low overall correlation of 0.18 (Figure 3.A). The PPD20V was within $8.3 \mu\text{g m}^{-3}$ of the TEOM at an hourly average 95 % of the time (sa). Over this three-day campaign, the sensor and TEOM showed significant disagreement (e.g., $\sim 20 \mu\text{g m}^{-3}$ difference on 10/3) intermittently. In some cases, not only was there a difference in the magnitude of the response but also in the response sign. During this the roadside comparison, RH and temperature had typical diurnal patterns for the southeast, ranging from 18-34, and 30-90%, respectively (Figure 3.D). 69% of the time the RH was below 70%, with 15% above 80% RH and no data above 90%. The error between the Shinyei and the TEOM was not significantly correlated with RH (R^2 0.007) or temperature (R^2 0.01).

Although much of this low correlation is due to errors in the Shinyei sensors, some of the inaccuracies may also lie in the TEOM (Allen et al., 1997), especially when using 1-hour averages. The concentrations were low at this location, which may cause a higher relative error in the TEOM since it is measuring smaller mass concentrations. Previous comparisons between the TEOM and the TSI sidepak, a portable nephelometer, showed an R^2 of only 0.75 at high concentrations of Arizona test dust ($75\text{-}125 \mu\text{g m}^{-3}$). In field studies, in urban and rural areas in Italy, average R^2 were 0.80. A relative humidity growth factor, based on dry and wet light scattering, was generated at each location. After correcting for this growth factor the R^2 increased on average 15% resulting in R^2 between 0.61 and 0.99. These were higher concentration ranges than those seen in Atlanta with 22 to $42 \mu\text{g m}^{-3}$ being the lowest concentration range experienced (Karagulian et al., 2012). Work comparing a TEOM and a nephelometer to the federal reference method (FRM) have shown linear correlations as low as 0.79 between the TEOM and the FRM and a linear correlation as low as 0.30 between the Nephelometer and FRM (Kashuba and Scheff, 2008). Overall, the link between light scattering signal and PM_{2.5} mass concentration is linked to the aerosol mass scattering efficiency

that in turn depends on particle size, composition and wavelength of light. As previously mentioned for urban air, not dominated by dust mass, the mass scattering is generally not highly variable (Carrico et al., 2003). Work in both Atlanta as well as rural China in a location influenced by coal burning (Xu et al., 2004) have relatively similar mass scattering efficiencies and taken together suggest uncertainties related to particle properties for volume light scattering instruments in urban-influenced areas are roughly 30%.

The low cost CO₂ sensor compared closely with the reference monitor with an inlet within a few feet of the sensor package. Hourly average data were used ($R^2 = 0.68$) over the three-day period (Figure 3.B). The two devices track closely with each other over the three-day time period except for two peaks on 10/3 and a peak near the initiation of testing on 10/1 detected by the reference monitor but not the low cost sensor. During these periods, for unknown reasons the sensor response was ~100 ppm lower than the reference analyser, and the discrepancy does not appear to be related to extreme temperature or humidity events as the ambient conditions were very close to those of the day before when data compared better.

The microAeth tracked trends well with the MAAP (Figures 3.C). The overall R^2 is 0.52, due to the fact that the microAeth filter strip became loaded and decreased in changes in light attenuation over time. This sensor requires manual filter changes, which creates challenges as the loading rate varies with atmospheric concentration and therefore the timing for conducting manual filter changes can be uncertain. If we compare during only the first 12 hours of sampling time, the R^2 is 0.99 and the concentration is within $0.21 \mu\text{g m}^{-3}$ 95% of the time.

3.1.2 Urban Background

Next, a comparison was performed on the roof top of the Ford Environmental Science and Technology Building (Figure 4, 5). The concentrations of PM_{2.5} seen on the roof were low (mean: $8 \mu\text{g m}^{-3}$), and the PPD60PV was the only sensor to achieve an R^2 value above 0.1, with an R^2 of 0.30. While the three PPD20V sensors do show agreeable precision with high correlations between them, they do not agree well with the TEOM (R^2 0.1 to 0.0). Therefore, no calibrations were performed between the sensors and the TEOM, allowing no errors to be calculated. In their current configuration, all of the low-cost particle sensors had low to no correlation with the TEOM while measuring lower urban background concentrations. Testing occurred during December during colder weather (average temperature = 12°C) with 50% of the data being above 70% RH and 38% above 80% RH.

3.1.3 High Ambient Concentrations

Lastly, the same sensor package that was deployed in Atlanta was deployed on a roof top in Hyderabad, India. The results from Hyderabad show higher average PM concentrations (1 hour averaged $72 \mu\text{g m}^{-3}$ range: $8\text{-}247 \mu\text{g m}^{-3}$) over the one-month deployment period (Figure 6). There are two large gaps in the data. From 2/3-2/7 the sensors were unplugged so no data were collected and from 2/10-2/25 the E-BAM was malfunctioning so these data were largely either not collected or not used due to instrument errors.

First we looked at the correlation between the PPD42NS and PPD20V sensors and the E-BAM which were all above the previously established cutoff of $R^2 \geq 0.1$ (PPD20V 1: 0.84, 2: 0.81, 3: 0.86, PPD42NS: 0.1). In this case we generated a calibration based on the first few days of data and applied it to later data. This shows how useful these sensors could be for future applications where a reference analyzer may not be available for the entire time period. A voltage-concentration relationship for the first half of the data (1/31-2/4 and 2/7-2/10) was generated and then applied it to the second half of the data (2/25-3/4). The relationships based on the first half are similar to those based on the full data set. Figure 6 shows the resulting sensor generated concentration compared with the E-BAM over time and Table 4 summarizes the results where d_{avg} is the average difference between the E-BAM and the sensor and s_d is the standard deviation of the differences. The average difference will be zero for the first period since this was the period used for calibration. The concentrations experienced during the second half of the deployment are lower than (1st period average: $91.1 \mu\text{g m}^{-3}$, range: $14.1\text{--}247 \mu\text{g m}^{-3}$, 2nd period average: $37.0 \mu\text{g m}^{-3}$, range: $3.2\text{--}96.8 \mu\text{g m}^{-3}$) during the data set that was used to calibrate the sensor signal which may lead to some of the error. The three PPD20V sensors have similar $2s_d$ around $30\text{--}40 \mu\text{g m}^{-3}$ but the average differences differ by $25 \mu\text{g m}^{-3}$ showing that the calibration generated for the PPD20V-2 underestimates PM concentrations during the second half of the study while the PPD20V-1 overestimates concentrations during the second half. There is no apparent consistent drift in the PPD20V sensor errors. During the calibration and application period the aerosol properties or sensor performance may be slightly different in addition to the previously noted concentration differences. The PPD60PV had larger errors than the PPD20Vs both during the calibration and application periods. The performance of the PPD42NS decreased significantly over time so 1/31-2/4 was used as the first calibration period and 2/7-2/10 was used as the application period. This calibration was not appropriate even during the 2/7-2/10 period with errors in the 100's of $\mu\text{g m}^{-3}$ showing either sensor drift, a decrease in sensor performance or other problems that are not understood at this time (Figure 6.C.3).

During this test the PPD60PV approaches saturation, as indicated by the exponential shape of the comparison where the PPD60PV reported concentration levels off at concentrations above about $100 \mu\text{g m}^{-3}$ in the Hyderabad environment (Figure 6.D). The resulting relationship between the E-BAM and PPD60PV is nonlinear due to this saturation. Gao et al. (Gao et al., 2015) observed saturation with the PPD42NS sensor operating under slightly higher concentrations in Xi'an China (hourly E-BAM average of $485 \mu\text{g m}^{-3}$ range: $77.0\text{--}889.0 \mu\text{g m}^{-3}$). We applied an exponential function to calibrate the PPD60PV against the E-BAM, whereas Gao et al. applied a fifth order polynomial to the PPD42NS signal that included temperature and humidity terms (Gao et al., 2015). The R^2 values generated for the full data set were very similar between the fifth order polynomial (0.64) and the exponential curve (0.62). An exponential function was applied as a calibration to the raw voltage signal data produced by the sensor, yielding Figure 6.E. The coefficients of determination were greater than 0.8 for the PPD20Vs in this study. The RH was 70% or below during 70% of the sample period with 15% of the data falling between 80 and 90% RH and no data included above 90% RH. The errors between the PPD60PV and PPD20Vs with the E-BAM were uncorrelated with RH ($R^2 < 0.04$). The error between PPD42NS and the TEOM had a low R^2 of 0.1. The PPD60PV sensor in India was the only sensor that was calibrated using a non-linear fit. We have also analyzed the lower concentration range of this data separately (Figure 7). The correlations are lower in all cases as shown during the urban background and Hyderabad ($< 100 \mu\text{g m}^{-3}$).

Simultaneous operation of three PPD20V sensors allowed comparison of sensors of the same type. The three PPD20V sensors have similar coefficients of determination (0.81-0.86) as shown in Figure 7. Also recorded in Table 4 are the slopes and intercepts of the calibrations whereas the graphs depict the post-calibration data (slope = 1, intercept = 0). PPD20V sensors 1 and 2 (Figures 8.A and 8.C) have similar calibrations with slopes of 0.45 and 0.46 while sensor 3 has a slope of 0.39. This slightly lower slope suggests the sensor is slightly more sensitive to changes in PM concentration. This is also suggested by the slightly higher R^2 of the 3rd PPD20V sensor. Although this is a small sample size of sensors, these widely differing calibrations show the need for individual calibration for each sensor, even those of the same model. In addition, these calibration equations differ from that generated at the roadside in Atlanta.

There are a variety of potential reasons for the inaccuracies in each concentration range. The Hyderabad concentration range seem more appropriate for the PPD20V, while at the low concentrations observed at the background roof site, the sensor agreed poorly with the reference measurements. Meanwhile, the PPD60PV agreed most closely with the reference TEOM at the background site and clearly can detect lower concentrations, which may be due to a combination of more sensitive electronics and/or optics. Additional work must occur to improve the performance of these sensors, especially at the roadside and background sites. However, at the high concentrations in Hyderabad above $200 \mu\text{g m}^{-3}$, the PPD20V sensors often became saturated (i.e. became insensitive to increases in ambient particle loading). This saturation occurred only 9 hours of the approximately 2-week period during which the measurements took place. The PPD42NS did not compare well at any concentration observed in this study and is likely due to the signal processing methodology employed, but also may be linked with sensor design and the sensitivity of the optical and electrical components..

A variety of factors affect light scattering, including particle size, shape, composition and relative humidity. The relationship between mass and light scattering is often highly correlated, but the relationship may be different in different locations and during different times of the year. This difference in the relationship has been shown in previous work using nephelometers (Chow et al., 2002). Comparisons for PM_{2.5} mass and light scattering with nephelometers are usually done using only the fine size fraction and under dry conditions, where the sample is heated to decrease RH to provide the most accurate results (Chow et al., 2002). Our study was done under ambient conditions, and we did not separate the smaller size fraction. Adding in a size separation device, to remove particles greater than $2.5 \mu\text{m}$, would significantly increase the cost and power consumption of particle sensor devices. In previous studies, total scattering has been compared with PM_{2.5} mass yielding linear relationships with high R^2 values (≥ 0.9) (Watson et al., 1991; Chow et al., 2002; Doran et al., 1998). Previous studies using low cost (\$150-\$2050) scattering PM sensors at US ambient concentrations ($\sim 0\text{-}30 \mu\text{g m}^{-3}$) have had max R^2 with FEMs of 0.8 and min R^2 of 0. This paper also looked into temperature and RH artifacts (Williams, 2014). It is possible the sensors could perform better in future studies in an improved enclosure with improved fan placement, or better light interference protection.

In previous studies, low RH and ambient RH PM_{2.5} light scattering has been compared with the effects of RH and has been relatively constant until 80% RH, with increasing errors after 80%. The largest errors occurred above 90% (Chow et al., 2002). Other studies have shown more dependence on RH, even at lower values with differences in scattering coefficients seen between 50 and 70%. The growth of the particles and therefore the scattering of the particles is variable in different locations

and over time as the composition of the particles is different, leading to more or less water uptake (Day and Malm, 2001). In addition, the manufacturer reports that the operating humidity range should stay at 95% or less (Shinyei Kaisha, 2002; Shinyei Technology Co., 2010, 2013). During all three tests, the RH in the sensing box was never above this value and was rarely above 90% and we did not attempt to correct our measurements for light scattering associated with water uptake. The temperature range reported by the manufacturer is 0-45 °C (Shinyei Technology Co., 2010; Shinyei Kaisha, 2002; Shinyei Technology Co., 2013), which was also not exceeded during testing. Although the temperature and humidity never exceeded the manufacturer-specified operation range, there could still be some dependence on RH and temperature as shown by Gao et al. (2015) in high concentration environments and also by Williams et al. (2015) in US lower concentrations environments. The electronics may be affected by temperature, as increased temperature increases the resistance in electronic circuits, which could affect the analog sensors.

3.1.4 Laboratory Comparison

During the chamber experiment the performance of the three Shinyei sensors were evaluated by comparison with a DustTrak monitor. One-minute averaged data were analyzed and the PPD20V yielded the highest correlation over all concentration ranges ($R^2 = 0.70$ from 0-50 $\mu\text{g m}^{-3}$ and $R^2 = 0.99$ from 0-500 $\mu\text{g m}^{-3}$) (Table 5). Note that the rest of the data in this paper were analyzed at 1 hour intervals leading to likely lower sensor noise than would be seen at 1 minute intervals.

The PPD60PV performed poorly at low concentrations in the lab ($R^2 = 0.20$ for 1 minute averages from 0-50 $\mu\text{g m}^{-3}$ in the lab). This was also seen in the ambient work on the roof top at similar conditions ($R^2 = 0.30$ for 1 hour averages from 0-38 $\mu\text{g m}^{-3}$ on the rooftop). At higher concentrations the coefficient of determination was higher ($R^2 = 0.87$, 0-500 $\mu\text{g m}^{-3}$) and the saturation that occurred during the India field experiments was not seen. This is likely due to the difference in chemical composition, mixing state and size distribution for the laboratory-generated incense versus in the ambient particulate matter in India.

Better agreement has been reported for the PPD42NS by Austin et al. 2015 ($R^2 = 0.66-0.99$, depending on particle diameter from 0-50 $\mu\text{g m}^{-3}$) than was seen in our laboratory results ($R^2 = 0.20$ from 0-50 $\mu\text{g m}^{-3}$). Wang et al. also reported much higher R^2 in their laboratory calibrations with incense ($R^2 = 0.95$ from 0-100 $\mu\text{g m}^{-3}$). This may be due to longer rolling averaging times (Austin et al., 2015), longer sampling time (2.5 hours) (Wang et al., 2015), differences in microcontroller signal processing, manufacturer variability in sensor production, and difference in comparison instruments (Austin et al., 2015; Wang et al., 2015).

The limit of detection (LOD) was also calculated in the lab by using the 95% confidence interval of the intercept after lab calibration on the 0-100 $\mu\text{g m}^{-3}$ range. The PPD42NS LOD calculated was 9.1 $\mu\text{g m}^{-3}$ which is higher than measured in Wang et al. (2015) (4.59 $\mu\text{g m}^{-3}$). The PPD20V has an LOD of 4.6 $\mu\text{g m}^{-3}$ while the PPD60PV has a higher limit of detection of 29 $\mu\text{g m}^{-3}$. Although the PPD60PV had performed better than the PPD20V at the lower rooftop concentrations, the poorer chamber performance may be due to the difference in averaging time, difference in aerosol properties, and differences in reference analyzers.

The challenge with optically-based PM sensors is that the actual response (i.e., sensor calibration) is largely a function of the actual properties of the ambient aerosol at the measurement location, including the size distribution and chemical composition. Further, the relationship can depend upon composition-related optical properties, and would also be RH dependent (Chow et al., 2002; Wang et al., 2015). Calibration to a mono- or poly-disperse calibration aerosol of a specific aerosol (e.g., sulfate or polystyrene latex (psl) or to another particle source such as incense, can lead to biases as the actual response in the field can be significantly different (Dacunto et al., 2015; Jiang et al., 2011; Wang et al., 2015; Austin et al., 2015). It is likely that the response to a laboratory generated aerosol will be much different to that in the field. In the end, calibration should be done with an aerosol similar to that being sampled. This is especially important given that the focus of this paper is on the use of an inexpensive sensor package to estimate emission factors where the focus is on the change in the local PM levels associated with changes in related gases. The dependence on aerosol properties will also impact the LOD as aerosol properties can be associated with concentration (e.g., periods of high concentrations will have different composition than at low concentrations).

4 Conclusions

This study undertook evaluating several low cost particle sensors in several field environments representing typical areas where additional air monitoring data would be desirable – urban near-highway environment in the United States, an urban background environment in the United States, and a highly polluted area of India. The sensors selected are easily procured commercially and are growing use by researchers building custom devices, incorporated in to turnkey sensor packages (e.g., AirBeam, Air Quality Egg), or being applied in build-your-own sensor kit packages for citizen science. Of the sensors studied, only the PPD20V appeared to have strong agreement with a reference monitor and that occurred during high concentrations experienced in Hyderabad, India (average: $72 \mu\text{g m}^{-3}$; $R^2 \geq 0.81$). Meanwhile, this same sensor had very weak agreement with a reference monitor next to a major roadway in Atlanta, Georgia (average= 21 ; $R^2 = 0.21$). Meanwhile, a different model sensor – the PPD60PV – displayed a nonlinear response at the high concentrations observed in India, whereas it did not display this nonlinearity at similarly high levels in a controlled laboratory test using incense as an emissions source. In addition, the PPD60PV sensor appeared to have moderate agreement (average= 8; $R^2 = 0.3$) with a reference monitor at the urban background location in Atlanta, Georgia, whereas the other sensors tested had effectively no relationship. Finally, although the PPD42NS sensor displayed good agreement with a reference during the laboratory test with incense smoke, the sensor had effectively no agreement with reference monitors in any of the measurement environments. These results suggest that specific sensors may have potential utility to quantify general ambient particulate matter trends, however, the importance of evaluating low cost particle sensors in their intended environment of use cannot be overstated.

30 Acknowledgements

This work was made possible by the NSF PIRE grant 1243535 and EPA Star grant R83503901. Thanks to J. Jeyaraman, R. Weber, L. King, and J. Hu at Georgia Tech and to J. Marshall at the University of Minnesota. The contents of this paper are solely the responsibility of the grantee and do not necessarily represent the official views of the US EPA or NSF. Further,

US EPA and NSF do not endorse the purchase of any commercial products or services mentioned in this paper. Although an EPA employee contributed to this article, the research presented was not performed or funded by and was not subject to EPA's quality system requirements. Consequently, the views, interpretations, and conclusions expressed in the article are solely those of the authors and do not necessarily reflect or represent EPA's views or policies.

5 References

- Allen, G., Sioutas, C., Koutrakis, P., Reiss, R., Lurmann, F. W., and Roberts, P. T.: Evaluation of the TEOM® method for measurement of ambient particulate mass in urban areas, *J. Air Waste Manage.*, 47, 682-689, 10.1080/10473289.1997.10463923, 1997.
- Ancelet, T., Davy, P. K., Mitchell, T., Trompetter, W. J., Markwitz, A., and Weatherburn, D. C.: Identification of particulate matter sources on an hourly time-scale in a wood burning community, *Environ. Sci. Technol.*, 46, 4767-4774, 10.1021/es203937y, 2012.
- Austin, E., Novosselov, I., Seto, E., and Yost, M. G.: Laboratory Evaluation of the Shinyei PPD42NS Low-Cost Particulate Matter Sensor, *PLoS ONE*, 10, e0137789, 10.1371/journal.pone.0137789, 2015.
- Bossche, J. V. d., Peters, J., Verwaeren, J., Botteldooren, D., Theunis, J., and De Baets, B.: Mobile monitoring for mapping spatial variation in urban air quality: Development and validation of a methodology based on an extensive dataset, *Atmos. Environ.*, 105, 148-161, <http://dx.doi.org/10.1016/j.atmosenv.2015.01.017>, 2015.
- Carrico, C. M., M. H. Bergin, and Xu, J.: Urban aerosol radiative properties: Measurements during the 1999 Atlanta Supersite Experiment, *Journal of Geophysical Research*, 108, 10.1029/2001jd001222, 2003.
- Cheng, Y.-H., and Lin, M.-H.: Real-Time performance of the microAeth® AE51 and the effects of aerosol loading on its measurement results at a traffic site, *Aerosol Air Qual. Res.*, 13, 1853–1863, 10.4209/aaqr.2012.12.0371, 2013.
- Chow, J. C.: Measurement methods to determine compliance with ambient air quality standards for suspended particles, *J. Air Waste Manage.*, 45, 320-382, 10.1080/10473289.1995.10467369, 1995.
- Chow, J. C., Watson, J. G., Lowenthal, D. H., and Richards, W.: Comparability between PM_{2.5} and particle light scattering measurements, *Environ. Monit. Assess.*, 79, 29-45, 2002.
- Dacunto, P. J., Klepeis, N. E., Cheng, K. C., Acevedo-Bolton, V., Jiang, R. T., Repace, J. L., Ott, W. R., and Hildemann, L. M.: Determining PM_{2.5} calibration curves for a low-cost particle monitor: common indoor residential aerosols, *Environ Sci Process Impacts*, 17, 1959-1966, 10.1039/c5em00365b, 2015.
- Day, D. E., and Malm, W. C.: Aerosol light scattering measurements as a function of relative humidity: a comparison between measurements made at three different sites, *Atmos. Environ.*, 35, 5169-5176, 2001.
- Doran, J. C., Bian, X., de Wekker, S. F. J., Edgerton, S., Fast, J. D., Hubbe, J. M., Shaw, W. J., Whiteman, C. D., Abbott, S., King, C., Leach, J., Mulhearn, M., Russell, C., Templeman, B., Wolfe, D., Archuleta, J., Elliott, S., Fernandez, A., Langley, D., Lee, J. T., Porph, W., Tellier, L., Chow, J., Watson, J. G., Coulter, R. L., Martin, T. J., Shannon, J. D., White, R., Martinez, D., Martinez, J. L., Mora, V., Sosa, G., Mercado, G., Pena, J. L., Salas, R., and Petty, R.: The IMADA-AVER boundary layer experiment in the Mexico City area, *B. Am Meteorol. Soc.*, 79, 2497–2508, 1998.
- EPA: National ambient air quality standards for particulate matter; Final rule Federal Register, 78, 3086-3287, 2013.
- EPA: List of designated reference and equivalent methods, www.epa.gov/ttn/air/criteria.html, 2015.
- Gao, M., Cao, J., and Seto, E.: A distributed network of low-cost continuous reading sensors to measure spatiotemporal variations of PM_{2.5} in Xi'an, China, *Environ. Pollut.*, 199, 56-65, <http://dx.doi.org/10.1016/j.envpol.2015.01.013>, 2015.
- GDOT: Permanent station 121-54 <http://trafficserver.transmetri.c.com/gdot-prod/tcdb.jsp?siteid=121-5474>, 2014.

- Health Effects Institute: Outdoor air pollution and health in the developing countries of asia: a comprehensive review, Special Report 18, 2010.
- Holstius, D. M., Pillariseti, A., Smith, K. R., and Seto, E.: Field calibrations of a low-cost aerosol sensor at a regulatory monitoring site in California, *Atmospheric Measurement Techniques*, 7, 1121-1131, 10.5194/amt-7-1121-2014, 2014.
- 5 Jiang, R. T., Acevedo-Bolton, V., Cheng, K. C., Klepeis, N. E., Ott, W. R., and Hildemann, L. M.: Determination of response of real-time SidePak AM510 monitor to secondhand smoke, other common indoor aerosols, and outdoor aerosol, *Journal of environmental monitoring : JEM*, 13, 1695-1702, 10.1039/c0em00732c, 2011.
- Karagulian, F., Belis, C. A., Lagler, F., Barbieri, M., and Gerboles, M.: Evaluation of a portable nephelometer against the Tapered Element Oscillating Microbalance method for monitoring PM_{2.5}, *Journal of Environmental Monitoring*, 14, 2145-2153, 10.1039/C2EM30099K, 2012.
- 10 Kashuba, R., and Scheff, P. A.: Nonlinear regression adjustments of multiple continuous monitoring methods produce effective characterization of short-term fine particulate matter, *Journal of the Air & Waste Management Association*, 58, 812+, 2008.
- Kumar, P., Morawska, L., Martani, C., Biskos, G., Neophytou, M., Di Sabatino, S., Bell, M., Norford, L., and Britter, R.: The rise of low-cost sensing for managing air pollution in cities, *Environ. Int.*, 75, 199-205, <http://dx.doi.org/10.1016/j.envint.2014.11.019>, 2015.
- 15 Laden, F., Schwartz, J., Speizer, F. E., and Dockery, D. W.: Reduction in fine particulate air pollution and mortality: extended follow-up of the harvard six cities study, *Am J. Resp. Crit. Care*, 173, 667-672, 10.1164/rccm.200503-443OC, 2006.
- McInnes, L., Bergin, M., Ogren, J., and Schwartz, S.: - Apportionment of light scattering and hygroscopic growth to aerosol composition, - 25, - 516, 1998.
- 20 Met One Instruments, I.: E-BAM particulate monitor operation manual E-BAM-9800 rev L, 2008.
- Miller, K. A., Siscovick, D. S., Sheppard, L., Shepherd, K., Sullivan, J. H., Anderson, G. L., and Kaufman, J. D.: Long-term exposure to air pollution and incidence of cardiovascular events in women, *New Engl. J. Med.*, 356, 447-458, 10.1056/NEJMoa054409, 2007.
- Nieuwenhuijsen, M. J., Donaire-Gonzalez, D., Rivas, I., de Castro, M., Cirach, M., Hoek, G., Seto, E., Jerrett, M., and Sunyer, J.: Variability in and agreement between modeled and personal continuously measured black carbon levels using novel smartphone and sensor technologies, *Environ. Sci. Technol.*, 49, 2977-2982, 10.1021/es505362x, 2015.
- 25 Pinto, J. P., Lefohn, A. S., and Shadwick, D. S.: Spatial Variability of PM_{2.5} in Urban Areas in the United States, *J. Air Waste Manage.*, 54, 440-449, 10.1080/10473289.2004.10470919, 2004.
- Puett, R. C., Hart, J. E., Yanosky, J. D., Paciorek, C., Schwartz, J., Suh, H., Speizer, F. E., and Laden, F.: Chronic fine and coarse particulate exposure, mortality, and coronary heart disease in the nurses' health study, *Environ. Health Persp.*, 117, 1697-1701, 10.1289/ehp.0900572, 2009.
- 30 Rood, M. J., D. S. Covert, and T. V. Larso: Hygroscopic properties of atmospheric aerosols in Riverside, California, *Tellus*, 39B, 383-397, 1987.
- Sensiron: Datasheet SHT1x (SHT10, SHT11, SHT15) Humidity and Temperature Sensor, 2010.
- 35 Shinyei Kaisha: Product specifications PPD20V, SP-30-E-99007 1-6, 2002.
- Shinyei Technology Co., L.: Specification sheet of PPD42NS, 2010.
- Shinyei Technology Co., L.: Product specifications PPD60PV-T2, SP-30-E-08003(V01) 2013.
- Snyder, E. G., Watkins, T. H., Solomon, P. A., Thom, E. D., Williams, R. W., Hagler, G. S. W., Shelow, D., Hindin, D. A., Kilaru, V. J., and Preuss, P. W.: The changing paradigm of air pollution monitoring, *Environ. Sci. Technol.*, 47, 11369-11377, 10.1021/es4022602, 2013.
- 40

- Steinle, S., Reis, S., Sabel, C. E., Semple, S., Twigg, M. M., Braban, C. F., Leeson, S. R., Heal, M. R., Harrison, D., Lin, C., and Wu, H.: Personal exposure monitoring of PM_{2.5} in indoor and outdoor microenvironments, *Sci. Total Environ.*, 508, 383-394, <http://dx.doi.org/10.1016/j.scitotenv.2014.12.003>, 2015.
- 5 Stevens, C., Williams, R., and Jones, P.: Progress on understanding spatial and temporal variability of PM(2.5) and its components in the Detroit Exposure and Aerosol Research Study (DEARS), *Environ Sci Process Impacts*, 16, 94-105, 10.1039/c3en00364g, 2014.
- Tiwari, S., Bisht, D. S., Srivastava, A. K., and Gustafsson, Ö.: Simultaneous measurements of black carbon and PM_{2.5}, CO, and NO_x variability at a locally polluted urban location in India, *Nat. Hazards*, 75, 813-829, 10.1007/s11069-014-1351-9, 2015.
- 10 USDA Forest Service: Smoke particulate monitors: 2006 update, 2006.
- Viana, M., Díez, S., Alastuey, A., Querol, X., and Reche, C.: Workplace exposure to traffic-derived nanoscaled particulates, *Journal of Physics: Conference Series*, 304, 012006, 10.1088/1742-6596/304/1/012006, 2011.
- 15 Wang, Y., Li, J., Jing, H., Zhang, Q., Jiang, J., and Biswas, P.: Laboratory Evaluation and Calibration of Three Low-Cost Particle Sensors for Particulate Matter Measurement, *Aerosol Science and Technology*, 49, 1063-1077, 10.1080/02786826.2015.1100710, 2015.
- Watson, J. G., Chow, J. C., Richards, L. W., Haase, D. L., McDade, C., Dietrich, D. L., Moon, D., and Sloane, C. S.: The 1989–1990 phoenix urban haze study, volume II: the apportionment of light extinction to sources, Prepared for Arizona Department of Environmental Quality, Phoenix, AZ, by Desert Research Institute, Reno, NV., DRI 8931.5F1, 1991.
- 20 Williams, R., A. Kaufman, T. Hanley, S. Garvey: Evaluation of Field-deployed Low Cost PM Sensors, EPA/600/R-14/464, 2014.
- Xu, J., Bergin, M. H., Greenwald, R., Schauer, J. J., Bergin, M., Shafer, M. M., Jaffrezo, J. L., and Aymoz, G.: Aerosol chemical, physical, and radiative characteristics near a desert source region of northwest China during ACE-Asia, *Journal of Geophysical Research*, 109, 10.1029/2003jd004239, 2004.

Table 1: Low and midcost sensors discussed in this paper

Pollutant	Sensor	Cost (\$)	Technology	Specifications
PM	Shinyei PPD42NS	10	volume light scattering (digital output)	>1 μm
PM	Shinyei PPD20V	250	volume light scattering (analog output)	>1 μm
PM	Shinyei PPD60PV	250	volume light scattering (analog output)	>0.5 μm
CO ₂	COZIR GC-0010	120	non-dispersive infrared absorption	0 to 2,000 ppm
Temperature and RH	Sensirion SHT 15	40	band-gap displacement	-40 to 100 °C \pm < 0.5 °C
			capacitance	0 to 100% \pm 2%
BC	Aethlabs AE51	6,000	filter absorbance change	0 to > 1 mg BC m ⁻³ \pm 0.1 $\mu\text{g BC m}^{-3}$, 1 min avg.

Table 2: Sample locations, dates, reference instruments, and sensors deployed

Date	Location	Reference	Sensor Model
10/1/13-10/4/13	Atlanta Roadside (33.775560, 84.390950),	TEOM	Shinyei PPD20V
		Thermo Scientific 410i	COZIR GC-0010
		MAAP	microAeth
11/21/13-12/16/13	Atlanta Roof Top (33.779175, 84.395730)	TEOM	Shinyei PPD42NS
			Shinyei PPD20V (x3)
			Shinyei PPD60PV
1/30/14-2/10/14	Hvderabad. India (17.425798, 78.526814)	E-BAM	Shinyei PPD42NS
			Shinyei PPD20V (x3)
			Shinyei PPD60PV

Table 3: Results from comparison between PM sensors and reference instruments during deployments in India and Atlanta

Location (Reference instrument)	1-h Reference Concentration Range ($\mu\text{g m}^{-3}$)	1-h Reference Average Concentration ($\mu\text{g m}^{-3}$)	Temperature and RH Range ($^{\circ}\text{C}$, %)	PM Sensor Model (Shinyei)	R ²
Atlanta Roadside (TEOM)	10-32	21	18-35 30-89	PPD20V	0.18
Atlanta Rooftop- urban background (TEOM)	0.5-38	8	0-27 13-92	PPD42NS PPD20V 1 PPD20V 2 PPD20V 3 PPD60PV	0.02 0.00 0.09 0.00 0.30
Hyderabad (E-BAM)	8-247	72	18-41 13-91	PPD42NS PPD20V 1 PPD20V 2 PPD20V 3 PPD60PV ^a	0.10 0.83 0.81 0.86 0.59

^aRaw signal fit with exponential curve

^bStandard Error N/A for sensors with correlations <0.10 where calibration was not generated

Table 4: Shinyei PM sensor calibrations generated from first half of Hyderabad data and their accuracy during a second later period where Estimate PM=m*(raw sensor signal) + b

Sensors	Calibration Coefficients (PM=m*sensoroutput+b)		Errors	1st period (1/31-2/4, 2/7-2/10)	2nd period (2/25-3/4)
PPD42NS ^a	m	40.0	2 ^{Sd}	57.8	290.6
	b	13.3	d _{avg}	0.0	-149.0
PPD20V 1	m	0.45	2 ^{Sd}	40.5	39.8
	b	-75.5	d _{avg}	0.0	9.2
PPD20V 2	m	0.46	2 ^{Sd}	43.1	32.5
	b	-84.8	d _{avg}	0.0	-15.9
PPD20V 3	m	0.39	2 ^{Sd}	37.4	34.0
	b	-50.4	d _{avg}	0.0	-0.8
PPD60PV ^b	m	123	2 ^{Sd}	48.2	77.0
	b	2.8	d _{avg}	0.0	-21.9

^aThe performance of the PPD42NS significantly decreased over time. For this analysis the 1st period is 1/31-2/4 and the second analysis is 2/7-2/10

^bLogarithmic calibration: Estimate PM = $e^{\frac{y-f}{e}} + c$

Table 5: Laboratory coefficient of determination of Shinyei PM sensors with TSI DustTrak using puff of incense smoke in chamber

Sensor R ²	Concentration range (µg m ⁻³)				Limit of Detection
	0-500	0-200	0-100	0-50	(µg m ⁻³)
PPD42NS	0.80	0.73	0.54	0.20	9.1
PPD20V	0.98	0.94	0.85	0.70	4.6
PPD60PV	0.87	0.49	0.10	0.04	29

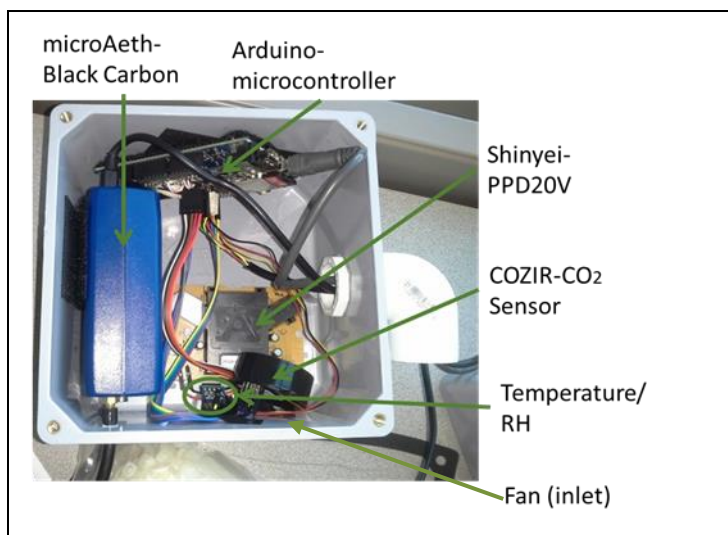


Figure 1: Sensor package design used during Atlanta roadside emissions factor testing

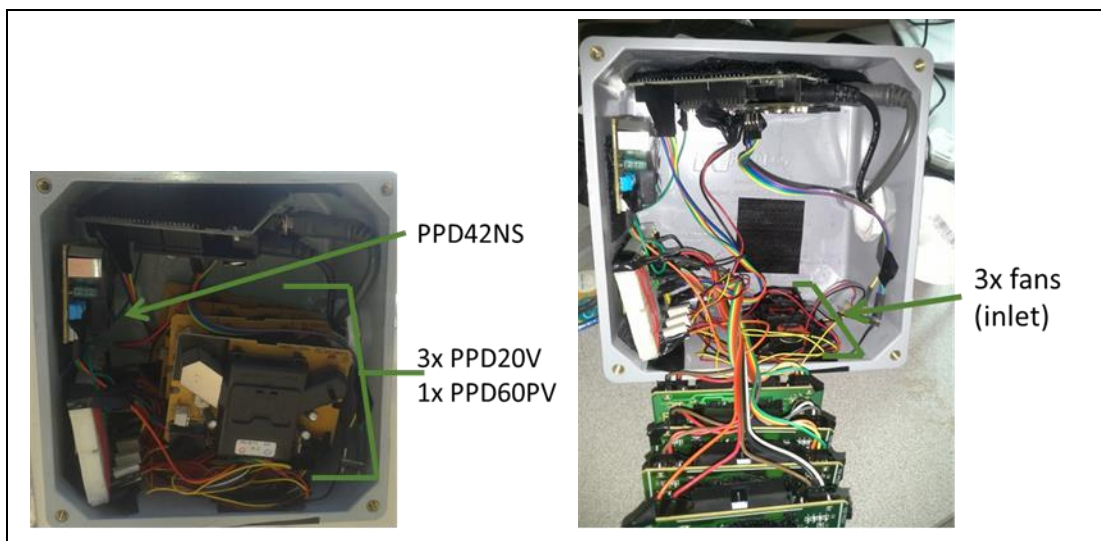


Figure 2: Shinyei particle sensor comparison box used during Hyderabad, India, and Atlanta rooftop testing

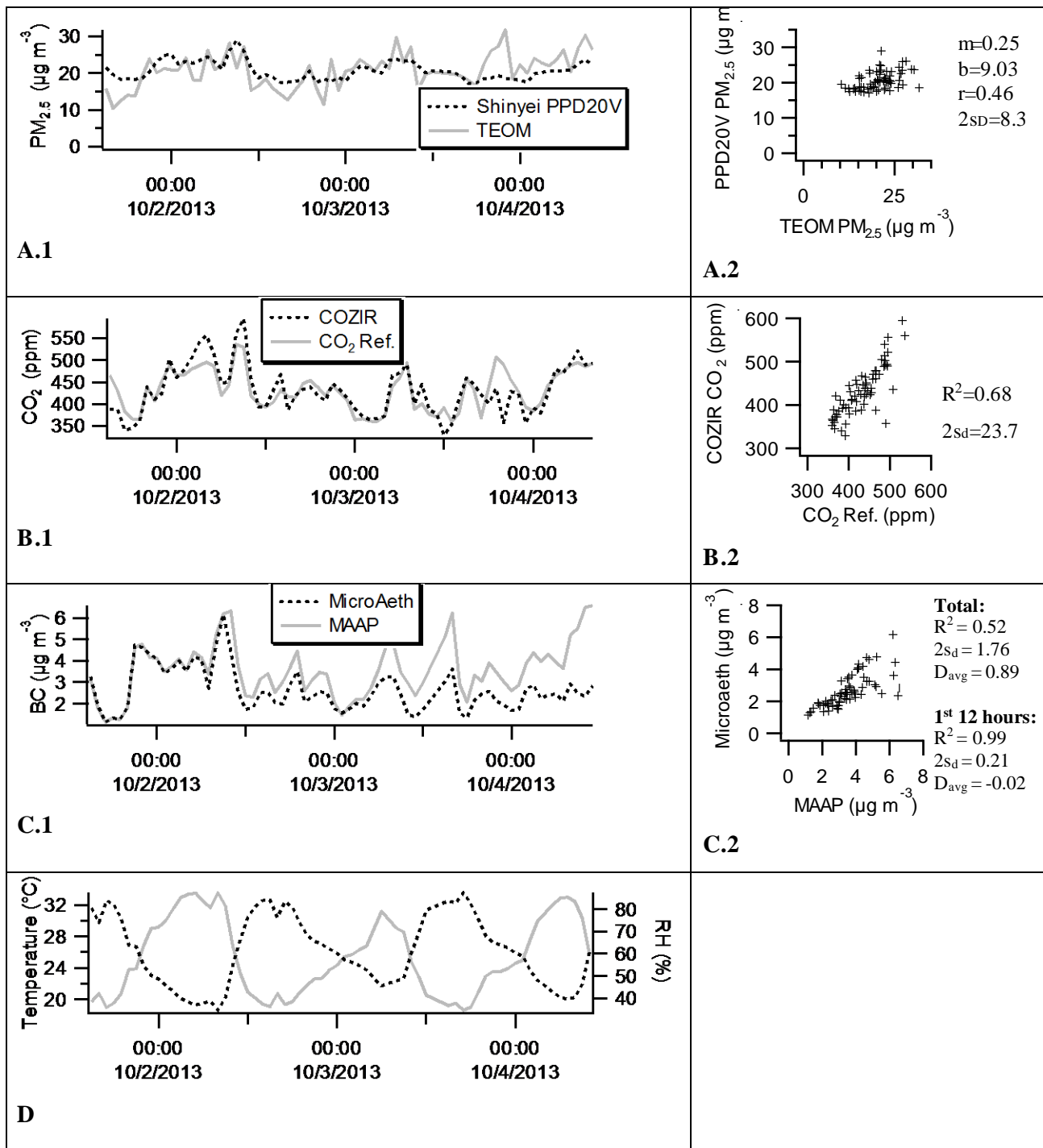


Figure 3: Atlanta roadside time series low cost sensors vs. reference analyzers a. PM, b. CO_2 , c. BC, d. temperature and RH from SHT 15 sensor inside sensor package

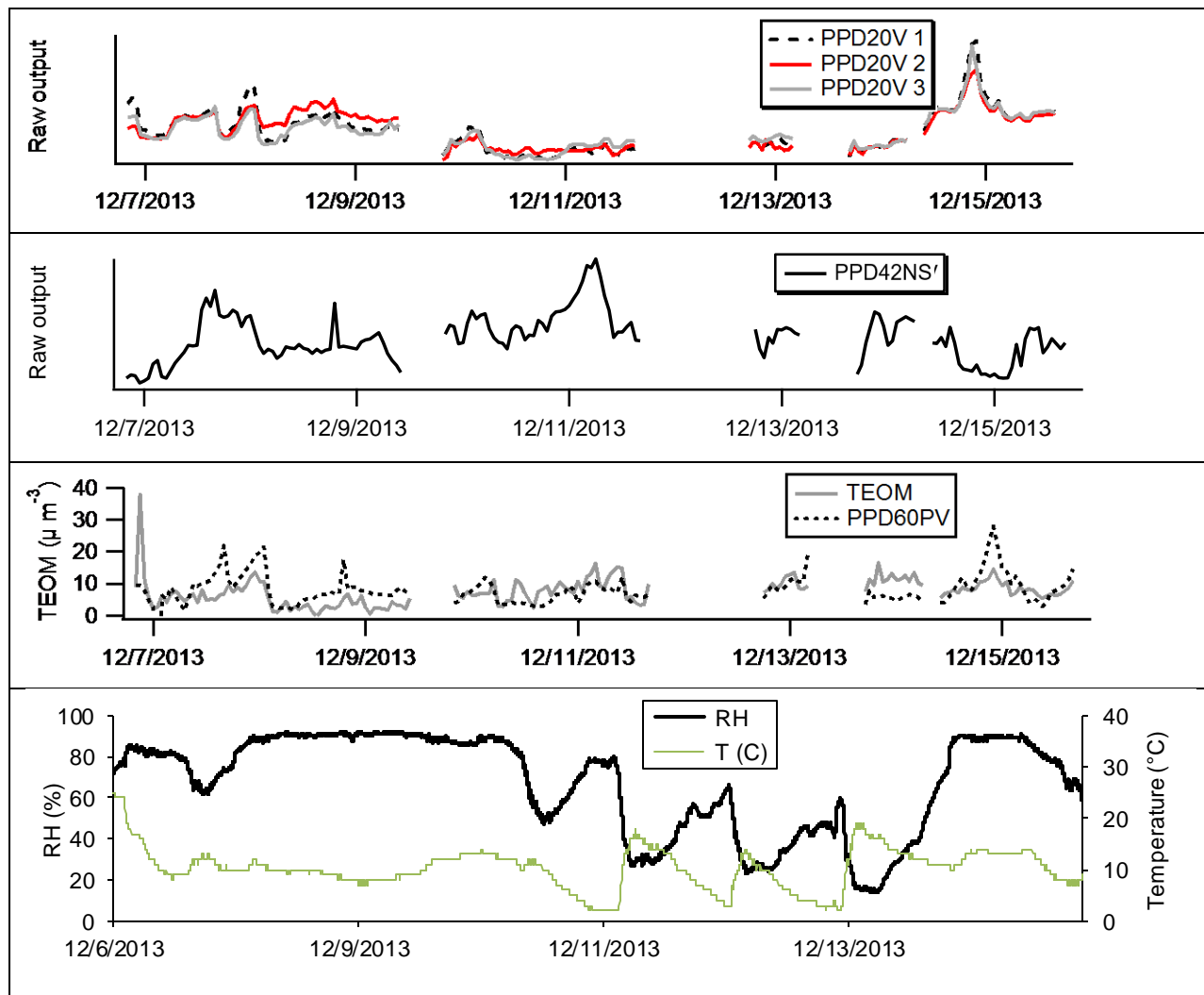


Figure 4: Rooftop comparison (portion of the full time series analyzed) shows the raw signals from the low cost particle sensors compared with the concentrations recorded by the TEOM on a one-hour average with temperature and RH

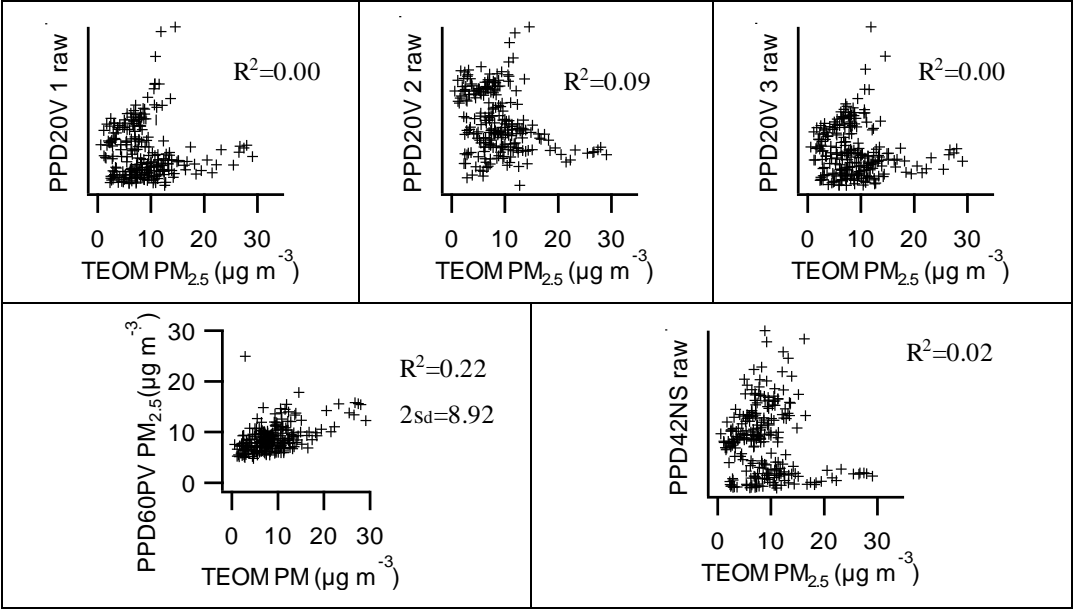
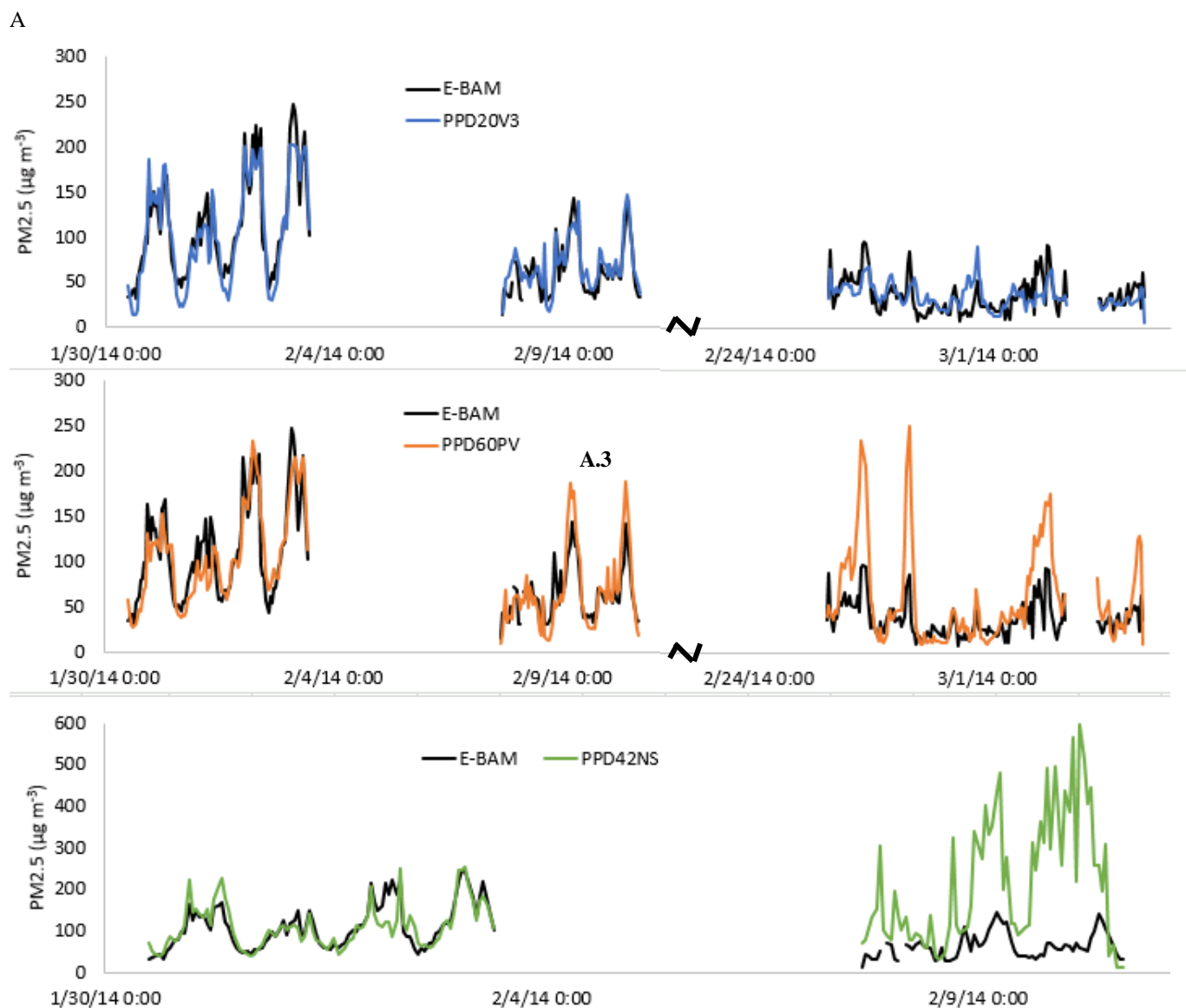


Figure 5. Atlanta rooftop comparison of Shinyei PM sensors with TEOM

*(Units have been left of PPD20V and PPD42NS sensors since no calibration was generated)



5 **Figure 6. Hyderabad, India Shinyei PM sensors comparison with E-BAM calibration generated during first half of time period and applied to second half**

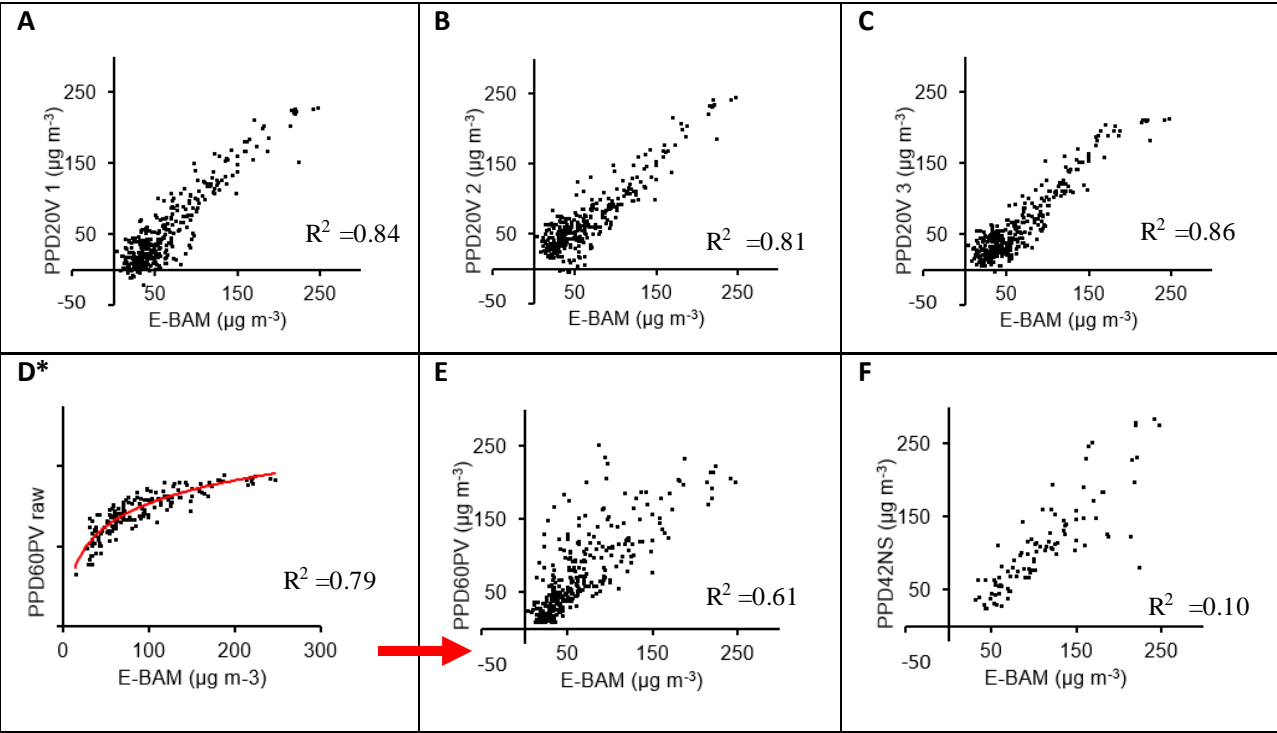


Figure 7: Correlation results from sensor and E-BAM comparison in Hyderabad, India

5 * Raw PPD60PV output-exponential fit ($\text{Shinyei} = a \cdot \ln(\text{E-BAM}) + b$)

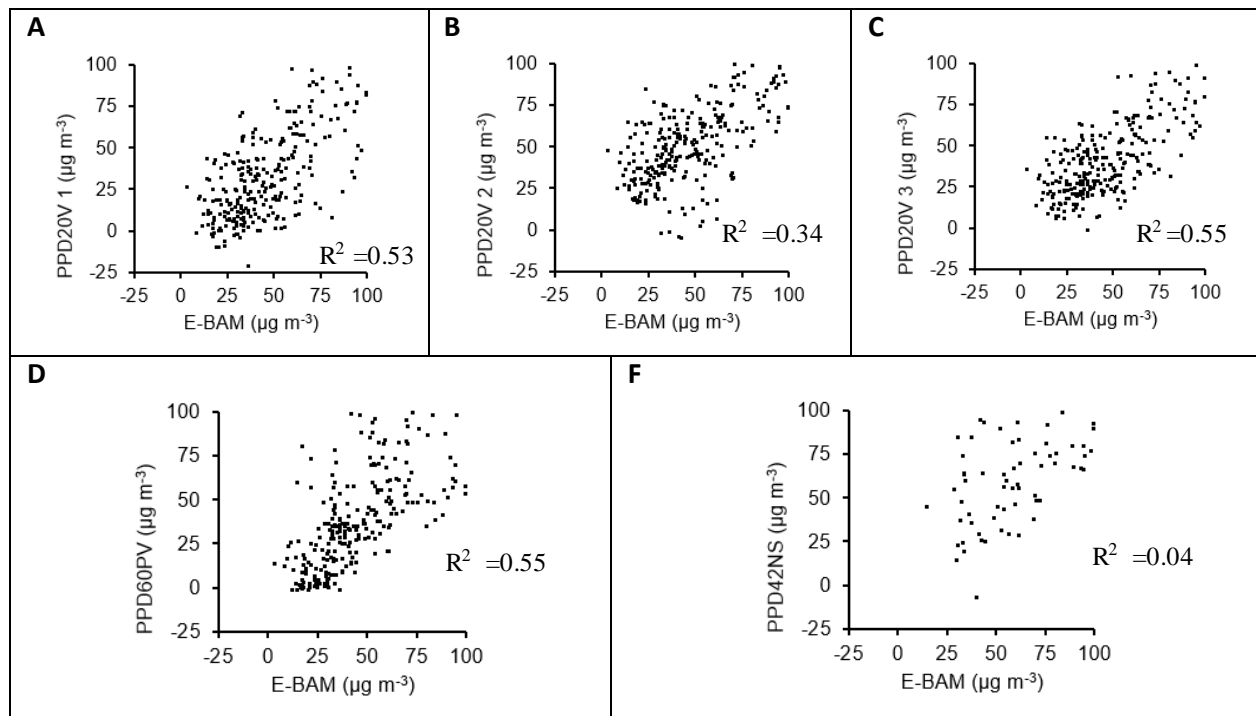


Figure 8: Low concentration (0-100 µg m⁻³) sensor correlations: results from sensor deployment in Hyderabad, India

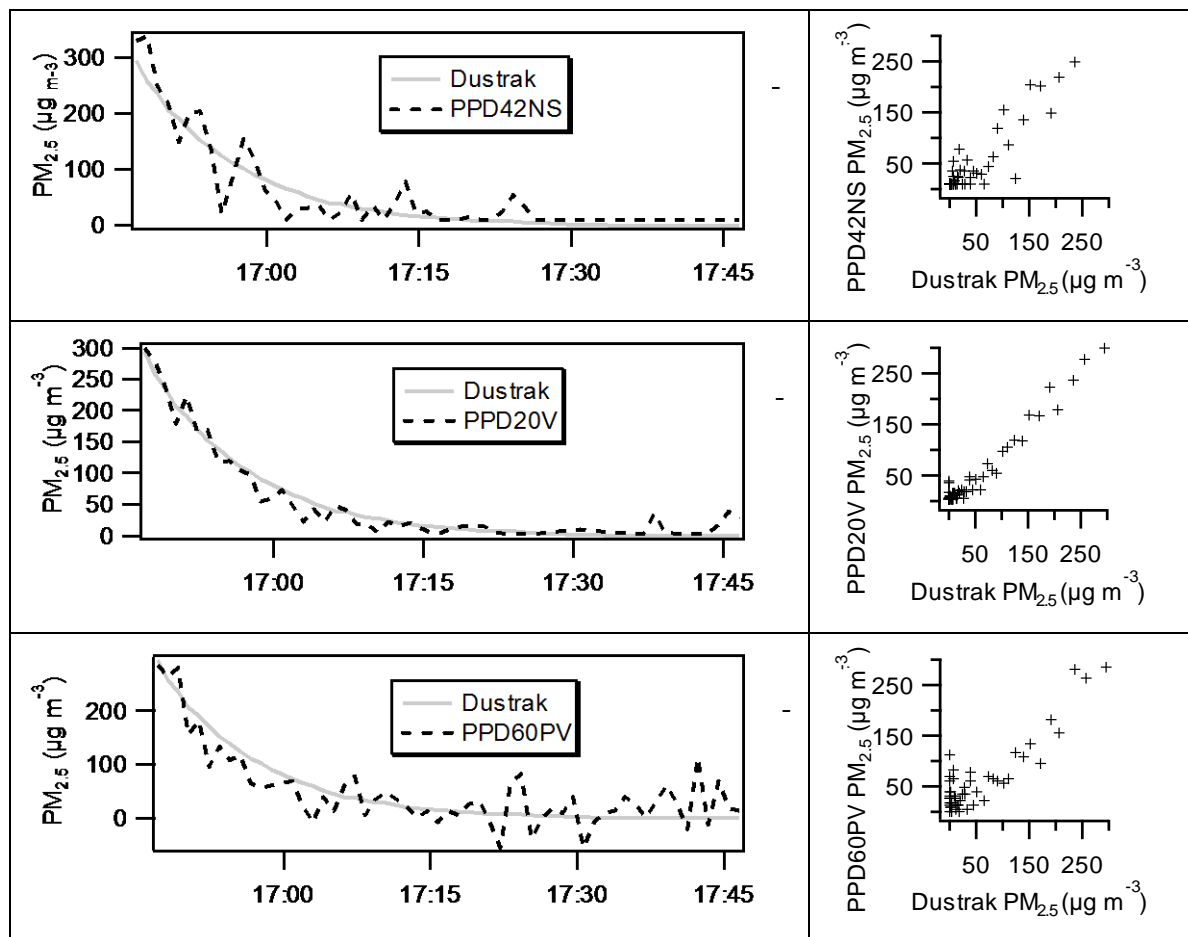


Figure 9. Chamber test comparison of Shinyei PM sensors with Dustrak using puff of incense smoke